Histol Histopathol (2010) 25: 1-14

http://www.hh.um.es

Histology and Histopathology

Cellular and Molecular Biology

Distribution of components of basal lamina and dystrophin-dystroglycan complex in the rat pineal gland: differences from the brain tissue and between the subdivisions of the gland

Zsolt Bagyura, Károly Pócsai and Mihály Kálmán

Department of Anatomy, Histology and Embryology, Semmelweis University, Budapest, Hungary

Summary. The pineal gland is an evagination of the brain tissue, a circumventricular neuroendocrine organ. Our immunohistochemical study investigates basal lamina components (laminin, agrin, perlecan, fibronectin), their receptor, the dystrophin-dystroglycan complex (ß-dystroglycan, dystrophin utrophin), aquaporins (-4,-9) and cellular markers (S100, neurofilament, GFAP, glutamine synthetase) in the adult rat corpus pineale. The aim was to compare the immunohistochemical features of the cerebral and pineal vessels and their environment, and to compare their features in the distal and proximal subdivisions of the so-called 'superficial pineal gland'. In contrast to the cerebral vessels, pineal vessels proved to be immunonegative to α1-dystrobrevin, but immunoreactive to laminin. An inner, dense, and an outer, loose layer of laminin as two basal laminae were present. The gap between them contained agrin and perlecan. Basal lamina components enmeshed the pinealocytes, too. Components of dystrophin-dystroglycan complex were also distributed along the vessels. Dystrophin, utrophin and agrin gave a 'patchy' distribution rather than a continuous one. The vessels were interconnected by wing-like structures, composed of basal lamina-components: a delicate network forming nests for cells. Cells immunostained with glutamine synthetase, S100-protein or neurofilament protein contacted the vessels, as well as GFAP- or aquaporin-immunostained astrocytes. Within the body a smaller, proximal, GFAP-and aquaporin-containing subdivision, and a larger, distal, GFAP-and aquaporin-free subdivision could be distinguished. The vascular localization of agrin and utrophin, as well as dystrophin, delineated vessels unequally, preferring the proximal or distal end of the body, respectively.

Key words: Agrin, Perlecan, Utrophin, Aquaporin, GFAP

Offprint requests to: M. Kalman, Department of Anatomy, Histology and Embryology, Semmelweis University, Tüzoltó 58, Budapest, H-1094, Hungary. e-mail: kalman@ana.sote.hu

Introduction

The pineal gland develops as an evagination of the neural tube. During phylogeny, the pineal develops from a photoreceptive organ into a gland secreting the hormone melatonin under control of light from the lateral eyes. The organ in rodents is composed of a superficial and a deep portion, connected via an intermediate portion, the pineal stalk (Vollrath, 1981; Heidbüchel and Vollrath, 1983; Møller and Baeres, 2002). Our present study focuses on the major, superficial part. Although it appears as an extrusion of the brain tissue, the pineal body has a special structure adapted to its functions.

The parenchymal cells of the mammalian pineal gland are hormone-producing pinealocytes, interstitial glial cells, and perivascular phagocytes. In some species, neurons and peptidergic neuron-like cells are present (Møller and Baeres, 2002). Interstitial cells in the proximal region of the superficial portion show immunoreactivity to GFAP (Møller et al., 1978b; López-Muñoz et al., 1992ab; Suzuki and Kachi, 1995), while those in the distal region are immunonegative to it. Whereas in the brain substance connective tissue is confined to the wall of vessels, the pineal body is penetrated from the pia mater by connective tissue

septae containing capillaries with fairly wide perivascular spaces. These septae separate cords of parenchymal cells. Light information is conducted to the pineal gland *via* extracerebral sympathetic and parasympathetic pathways, beside the central visual ones (Lerner et al., 1959; Ganguly et al., 2002). Similar intrusion of postganglionic vegetative fibres did not occur in other part of the brain. The pineal body has its separate blood circulation, since it receives arteries from the posterior choroidal artery, a branch of the posterior cerebral artery, and it is drained by veins into the great cerebral vein. Its vascular structure is different from the brain tissue. The capillaries are permeable in every species for low and high molecular weight tracers (Møller et al., 1978a; Møller and van Veen, 1981; Welsh and Beitz, 1981) in contrast to the strictly sealed blood-brain barrier of cerebral vessels. The wide perivascular spaces have been mentioned. The lack of blood-brain barrier is characteristic of the circumventricular organs (except for the subcommissural one) which the pineal gland belongs to according to several authors (e.g. Palkovits, 1986; Vígh et al., 2004).

Therefore, there are differences between the pineal gland and the brain tissue in their function (i.e. the pineal is an endocrine gland), vascular structure (e.g. pineal vessels have no blood-brain barrier), and connective tissue elements (absent from the brain substance, except for vessels). The question is how these differences are reflected by differences in immunohistochemical reactions against the components of basal lamina and dystrophin-dystroglycan complex.

The main adhesive component of the basal lamina is the laminin, which is important for brain vascularization, histogenesis, and post-lesion processes. It consists of three polypeptide chains (α, ß, γ). The chains have isoforms, therefore by their combinations multiple types of laminins can be formed, until now 15 types have been described, being specific for localisation and function (Colognato and Yurchenko, 2000; Libby et al., 2000). Collagen of type 4, the heparansulfate proteoglycan perlecan, agrin, nidogen, entactin are also components of the basal lamina. The basal lamina is bound by cellular laminin receptors such as integrins and dystroglycan.

Dystroglycan was identified first in skeletal muscle, as a component of the dystrophin-glycosamin complex (DGC), but later also in other tissues, including brain (for an early review, see Henry and Campbell, 1996). Durbeej et al. (1998a,b) found that dystroglycan is a ubiquitous cell surface receptor involved in linking cells to basement membranes in adult tissues. It is required for the stabilization of vascular structure, and for the maturation and functional integrity of the blood-brain barrier (Tian et al., 1996; Jancsik and Hajós, 1999; Nico et al., 2001, 2003, 2004; Zaccaria et al., 2001).

Dystroglycan is encoded by a single gene and cleaved by post-translational processing into two proteins: α- and ß-dystroglycan- (Ibraghimov-Beskrovnaya et al., 1992; Smalheiser and Kim, 1995). The α-dystroglycan is a highly glycosylated extracellular protein which binds to laminin and other basal lamina components, e.g. agrin, perlecan. ß-dystroglycan is a transmembrane protein that anchors α-dystroglycan to the cell membrane. The other end of ß-dystroglycan forms a complex with dystrobrevin (α1, α2 or ß), syntrophin (α1, α2, ß, γ1 or γ2), and different dystrophin isoforms (or utrophin). The dystrophin component connects actin to the ß-dystroglycan, whereas dystrobrevin sustains a connection with intracellular signalization systems. (For a more detailed description, see Chamberlain, 1999; Moukhles and Carbonetto, 2001; Culligan and Ohlendieck, 2002; Ehmsen et al., 2002; Amiry-Moghaddam et al., 2004; Warth et al., 2004, 2005).

The dystroglycan complex, first of all its syntrophin component, is responsible for the distribution and anchoring of the water-pore channel protein, aquaporin-4 (AQP4, Neely et al., 2001; Amiry-Moghaddam et al., 2003a,b, 2004; Nico et al., 2003, 2004; Warth et al., 2004, 2005). In the mammalian brain (except for the choroid plexus), the prevalent aquaporin proved to be AQP4 (Hasegawa et al., 1994; Jung et al., 1994; Frigeri et al., 1995), which occurs mainly in astroglial end feet, whereas AQP9 (Badaut and Regli, 2004) is localized to the astrocyte perikarya and processes. They play a crucial role in volume homeostasis (Venero et al., 2001; Agre et al., 2002; Vajda et al., 2002; Agre and Kozono, 2003). Nico et al. (2001) found AQP4 to be a marker of the maturation and integration of the blood-brain barrier. Therefore, we extended the investigations to cover aquaporin-4 and 9.

The present immunohistochemical study investigates basal lamina components (laminin, agrin, perlecan), the dystrophin-dystroglycan complex (ß-dystroglycan, dystrophin isoforms, utrophin, dystrobrevin and syntrophin), aquaporins (-4,-9), connective tissue elements fibronectin and collagen type I, glial markers (glial fibrillary filament protein, i.e. GFAP, glutamine synthetase and S-100 protein), and neural marker neurofilament protein in the superficial portion of the adult rat corpus pineale. Besides description, the aim of the study is to compare the immunohistochemical features of the pineal blood vessels to that of cerebral vessels. Since these latter ones have been investigated extensively (see citations in the Introduction and Discussion), their features are cited from the literature, and have not been displayed in figures repeatedly here.

Materials and methods

Animals

Adult rats (Wistar) weighing 250 to 300 g of either sex were used. The animals had access to food and water *ad libitum,* and were kept in an 12/12 h light/darkness schedule. All experimental procedures were performed in accordance with the guidelines of European

Communities Council Directive (86/609/EEC).

Fixation and sectioning

The animals were deeply anesthetized with ketamine and xylazine (20 and 80 mg/kg, respectively, i.m.) and perfused through the aorta with 100 ml 0.9% sodium chloride followed by 300 ml 4% paraformaldehyde in 0.1 M phosphate buffer (pH 7.4). After perfusion, brains were removed and post-fixed in the same fixative for 3 days at 4°C. The superficial pineal gland (in sagittal plane) was cut into serial sections (thickness 100 μm) by vibratome (Leica VT 1000S) and stored in PBS (phosphate buffered saline, Sigma) at 4°C.

Immunohistochemistry

Primary immunoreagents are listed in Table 1. Free floating sections were pre-treated with normal goat serum, or in the case of dystrobrevins, horse serum, diluted to 20% in PBS for 90 min to block the non-specific binding of antibodies. This and the following steps were followed by an extensive wash in PBS (30 min, at room temperature). Primary antibodies were diluted as described above in PBS containing 0.5% Triton X-100 and 0.01% sodium azide. Sections were incubated for 40 h at 4°C. Fluorescent secondary antibodies (Table 2) were used at room temperature for 3h. The sections were finally washed in PBS (1h, at room temperature), mounted onto slides, coverslipped in a mixture of glycerol and bi-distilled water (1:1), and sealed with lacquer. Control sections were installed by the omission of the primary antibody. No structure-bound fluorescent labelling was observed in these specimens.

Double-labeling immunofluorescent reactions

Double-labelling experiments were performed where antibodies of different origin (e.g. mouse *versus* rabbit) were available against the components labelled together. In the case of anti-rat antibodies either Alexa Fluor 488- or rhodamin-containing secondary antibody was applied, to make possible combinations with either Cy^3 conjugated anti-mouse or FITC-conjugated anti-rabbit antibodies. For the same purpose, two different GFAP

Table 1. The primary antibodies applied in the study.

Against	Type	Supplier	Code Nr.	Dilution
ß-Dystroglycan	Mouse*	Novocastra, Newcastle-upon-Tyne, England	ncl-b-dg	1:100
Dystrophin (Dys2)	Mouse*	Novocastra, Newcastle-upon-Tyne, England	ncl-dys2	1:10
α1-distrobrevin	Goat**	Santa Cruz Biotechnology, Santa Cruz, Ca, USA	(v-19) sc-13812	1:100
ß -distrobrevin	Goat**	Santa Cruz Biotechnology, Santa Cruz, Ca, USA	(m-15) sc-13815	1:100
α1-Syntrophin	Rabbit**	Sigma, San Louis, Mo, USA	s4688	1:100
Utrophin	Mouse*	Novocastra, Newcastle-upon-Tyne, England	ncl-drp2	1:10
Aquaporin-4	Rabbit**	Sigma, San Louis, Mo, USA	a5371	1:200
Aquaporin-9	Rabbit**	Alpha Diagnostics, San Antonio, Tx, USA	cataq p91-a	1:100
Neurofilament	Mouse*	Boehringer, Mannheim	bf 10	1:100
S100	Rabbit**	Sigma, San Louis, Mo, USA	s-2644	1:100
Glutamine-synthetase	Mouse*	Transduction Laboratories, Erembodegem, Belgium	610518	1:100
GFAP	Mouse*	Novocastra, Newcastle, United Kingdom	ga5	1:100
GFAP	Rabbit**	DAKO, Glostrup, Denmark	z0334	1:100
Collagen type I	Mouse*	Sigma, San Louis, Mo, USA	c 2456	1:100
Fibronectin	Rabbit**	Sigma, San Louis, Mo, USA	f 3648	1:100
Laminin 1	Rabbit**	Sigma, San Louis, Mo, USA	l 9393	1:100
Perlecan	Rat*	Santa Cruz Biotechnology, Santa Cruz, Ca, USA	sc-33707	1:100
Agrin	Mouse*	Biomol GmbH, Hamburg, Germany	agr-131	1:100

*: monoclonal; **: polyclonal

Table 2. The secondary antibodies applied in the study.

Conjugated with	Against	Type	Absorbead light/ Emitted light (nm)	Supplier	Code Nr.	Dilution
Fluorescein (FITC)	Rabbit	Donkey	492 (blue) / 520 (green)	Jackson Immunoresearch Laboratories, West Grove, Pa, USA	711-095-152	1:250
Fluorescein (FITC)	Goat	Donkey	492 (blue) / 520 (green)	Jackson Immunoresearch Laboratories, West Grove, Pa, USA	705-093-003	1:250
Alexa Fluor 488	Rat	Donkey	495 (blue) / 519 (green)	Invitrogen, Carlsbad, Ca, USA	a21208	1:500
Cy3	Mouse	Donkey	550 (green) / 570 (red)	Jackson Immunoresearch Laboratories, West Grove, Pa, USA	715-165-150	1:250
Rhodamin	Rat	Goat	550 (green) / 570 (red)	Thermo Fischer Scientific Inc., Rockford, Il, USA	31680	1:250

antibodies (polyclonal rabbit and monoclonal mouse) were used. Otherwise the protocol was similar to before.

Confocal laser scanning microscopy and digital imaging

Slides were photographed by a DP50 digital camera mounted on a Olympus BX-51 microscope (both from Olympus Optical Co. Ltd, Tokyo, Japan), or, in the case of double labellings, by a Radiance-2100 (BioRad, Hercules, CA) confocal laser scanning microscope. Green and red colours on the photomicrographs correspond to the fluorescent dyes as shown in Table 2. Digital images were processed using Photoshop 9.2 software (Adobe Systems, Mountain View, CA) with minimal adjustments for brightness and contrast.

Results

The pineal vessels were immunoreactive to laminin throughout the gland, although less intensely than the meningeal vessels (Fig. 1a,b). Around the vessels the 'background' staining was quite intense. At higher magnification the lumina of the vessels were recognizable (Fig. 1c). In the 'background' higher magnification revealed a delicate network, in which the vessels were interconnected by wing-like structures. Dystroglycan immunoreactivity labelled vessels in the major part of the pineal body (Fig. 1e,f), mainly around its proximal and distal poles, but less consequently than laminin. Several vessels which were visualized clearly by immunostaining to laminin (Fig. 1d,e) were hardly or not recognizable following immunostaining against dystroglycan. Dystroglycan immunostaining revealed a similar background 'network' as that of laminin did. Immunostaining against another basal lamina component, perlecan, also visualized both vessels, in even distribution throughout of the organ (Fig. 1g,h) and a network around them.

Whereas laminin, dystroglycan, and perlecan could be detected in vessels in any area of the pineal body, other basal lamina- and dystroglycan complex-components proved to be unevenly localized. Dystrophin immunopositive vessels were found only around the distal pole, opposite to the stalk (Fig. 2a), although dystrophin immunopositivity was found in the background network throughout the body (Fig. 2b). An even smaller number of the vessels were immunoreactive to utrophin. These vessels were found mainly near the stalk (Fig. 2c), as well as vessels immunopositive to agrin, a basal lamina component (Fig. 2e). Of the vessels only segments were labelled. Otherwise utrophin and agrin were ubiquitous, forming networks (Fig. 2d,f) throughout the body, like the other substances described above, so their 'background' stainings were quite intense. Collagen I and fibronectin occurred only adjacent to the distal pole of the superficial pineal gland (Fig. 2g,h), near the surface. Neither syntrophin (at least no α1) nor dystrobrevin (either α1 or ß) was found.

When immunostainings were applied against glial and neural markers, cells immunoreactive to S100 and/or glutamine synthetase were distributed more or less evenly throughout the pineal gland. Most parenchymal cells in the pineal gland were S100 protein-immunopositive. Immunostaining of aquaporin-4, however, divided the organ into an immunopositive, proximal area, and a major, distal one, which proved to be negative (Fig. 3a). Their proportion was approximately 2 to 1, and the transition from the aquaporin immunopositive area to the immunonegative one seemed to be rather abrupt. The GFAP immunopositive cells occurred in a similar area as the aquaporin-4 positive ones. When double labelling against GFAP and neurofilament protein was applied, neurofilament immunopositive cells occupied the distal part of the body, with only a minimal overlap with the area of the GFAP-immunopositive astrocytes (Fig. 3b, c). No distribution of the above mentioned vascular immunoreactivities, however, coincided exactly with either the GFAP-immunopositive or -negative areas.

When laminin was co-labelled with dystroglycan (Fig. 4a,b), dystrophin (Fig. 4c), or utrophin (Fig. 4d), components of the dystrophin-dystroglycan complex, as well as with perlecan (Fig. 4e,d,f) or agrin (Fig. 4g,h), the observations were similar to each other. At lower magnification the vessels were marked by a continuous green or yellowish green colour, i.e. laminin predominated, whereas their environment was rather reddish, i.e. there the laminin immunostaining was less intense than that of the other component. Single labelling, however, proved that laminin (see Fig. 1a-c) does contribute to the formation of the background network, as well as the other components delineating vascular walls (see again Fig. 1e-h, and Fig. 2a-h). High-power objective distinguished two laminin-containing (green or yellowish) layers around vessels: an inner, dense one and an outer, loose one as two separate basal laminae. If they were decorated with different colours, the inner was green and the outer was yellow, and maybe the best demonstration of them is in Fig. 4b. The loose, discontinuous structure of the outer layer is visible in the inset of Fig. 4c, and Fig. 4f. The inner one was a vascular basal lamina below the endothelium. The outer one was supposed to belong to the pineal parenchyma. The gap between them contained perlecan and agrin (Fig. 4f,h), as well as dystroglycan (Fig. 4a inset, b), dystrophin (Fig. 4c inset) and utrophin (Fig. 4d) immunopositive substances, which attached in uneven patches from outside (i.e., contraluminally) to the basal lamina of the vessels.

Even when only single labelling was applied, cell contours sometimes appeared in the network around the vessels. In double-labelling studies the relationship of cells and basal lamina-components could be studied better, when cells were weakly stained and several of them attached to the outer basal lamina (Fig. 4b) or were surrounded by the fibres of the background network (Fig. 4f).

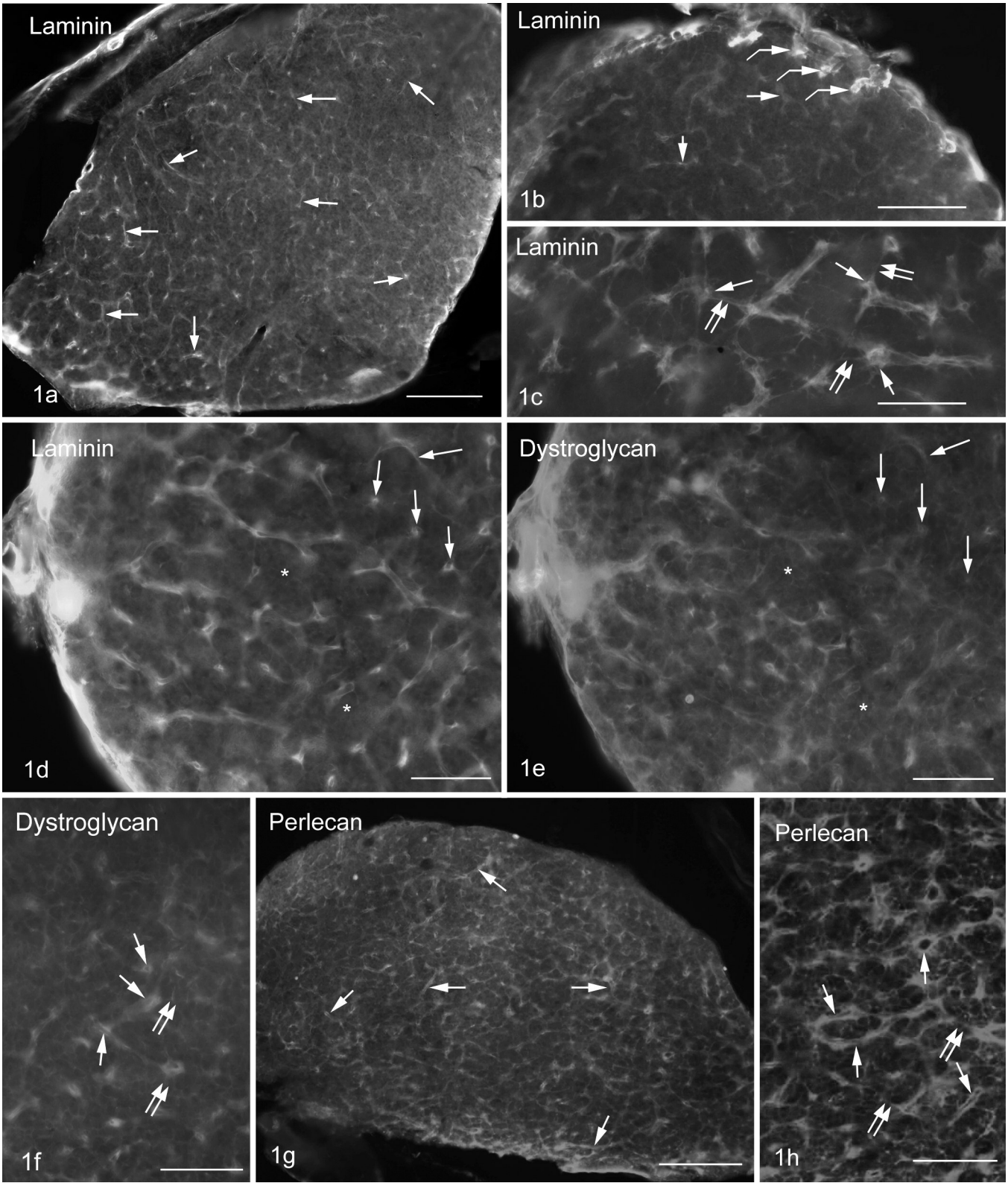

Fig. 1. Vessels visualized by immunohistochemical reactions against basal lamina- and dystroglycan-complex components in the pineal body. **a and b.** Laminin immunostaining (the original colour is green). The vessels (arrows) are visualized throughout the organ, although less intensely than where they enter the organ (broken arrows, panel **b**). **c.** Laminin immunostaining. At higher magnification luminae are recognizable (arrows). Note the delicate network interconnecting the vessels (double arrows). **d and e.** Laminin and dystroglycan immunostainings respectively (the original colours were green and red, respectively). Dystroglycan immunostaining visualizes some vessels (arrows) poorly as compared to laminin. The network (asterisks) around the vessels is recognizable at both immunostainings. **f.** Dystroglycan immunostaining (the original color is red), at higher magnification. The lumina of vessels are recognizable (arrows). Double arrows point to fine fiber-like structures which form a network around and between the vessels. **g.** Perlecan immunostaining (the original colour is red). Vessels (arrows) are delineated throughout the organ. **h.** Perlecan immunostaining (the original color is red), at higher magnification. The lumina of vessels are recognizable (arrows). Double arrows point to fine fiber-like structures which form a network around and between the vessels. Scale bars: a, g, 250 μm; b, d-f, 200 μm; c, h, 100 μm.

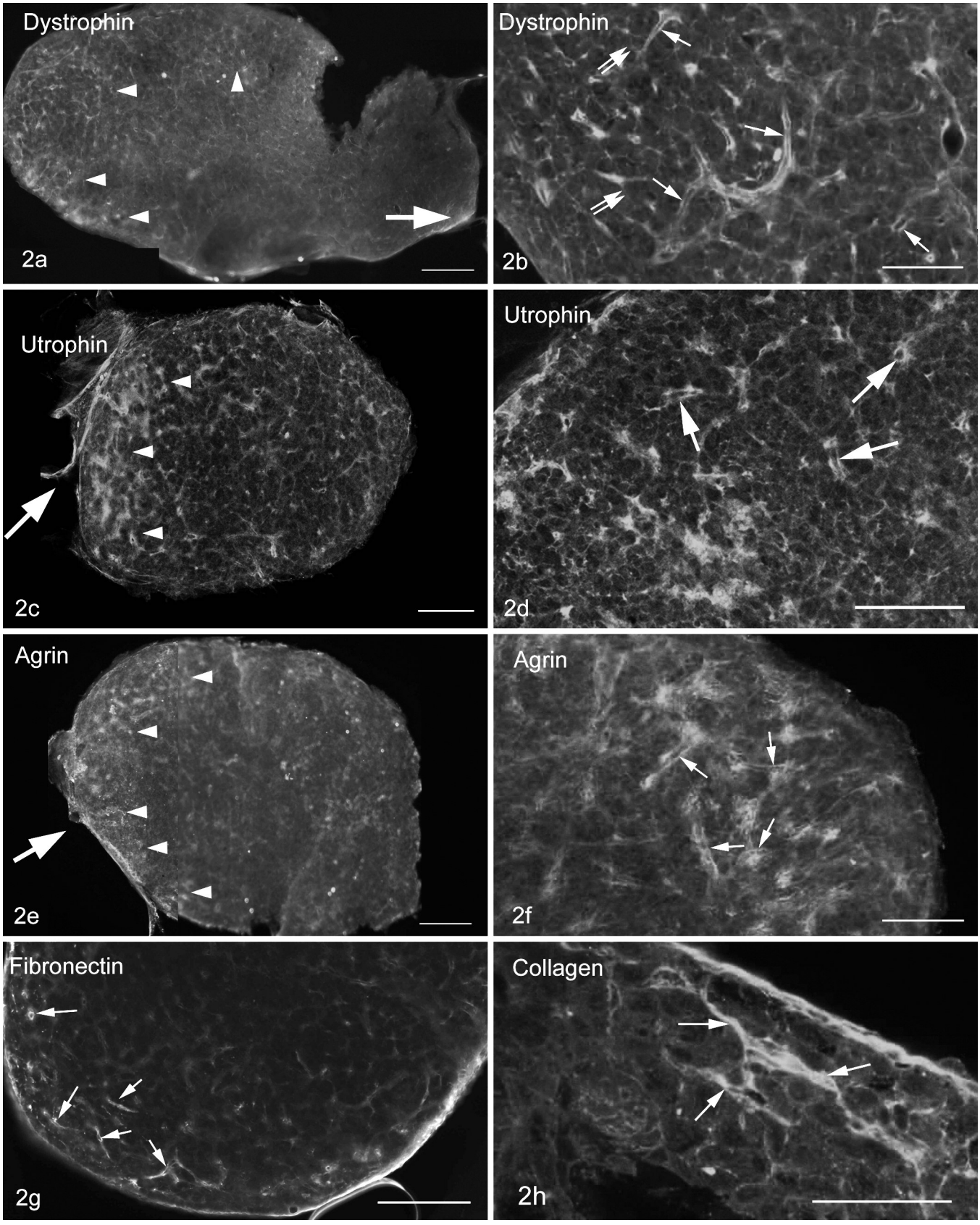

Fig 2. Uneven distributions of vascular immunoreactivities in the pineal body. **a and b.** Dys2 antibody visualizes vessels on the distal area (arrowheads) of the pineal body, opposite the stalk (thick arrow). The original colour was red. In panel **b**, at higher magnification the vessels (arrow) and the branches of the interconnecting (double arrows) are clearly recognizable. **c.** Utrophin-immunostained vessels are also most frequent (arrowheads) at the stalk (thick arrow). Panel **d**) reveals lumina of vessels. Note the network around. The original colour was red. **e and f.** Immunostaining against agrin shows similar distribution like the previous ones. The original colour was red. **g and h.** Fibronectin and collagen I immunostainings label vessels (arrows) only adjacent to the surface, on the distal end, opposite the stalk. The original colours were green and red, respectively. Scale bars: a, c, e, g, 250 μm; b, d, f, 100 μm; h, 50 μm.

As was mentioned above, the majority of cells were S100-immunopositive, but neurofilament protein and glutamine synthetase immunoreactive cells were also numerous. Co-localization between glutamine synthetase and S100-protein was infrequent. Either cell type had vascular contacts (Fig. 5a-f), including GFAP-immunopositive cell processes and aquaporin-4 immunopositive cells. These latter contacts however, were formed not so regularly that the course of vessels could have been followed. It is to be noted that aquaporin-4 was evenly distributed in the cells displaying their stellate form (Fig. 5d), in contrast to the cerebral localization in end-feet. At least a part of these cells also proved to be immunoreactive to GFAP (Fig. 5e). Immunohistochemical reaction to aquaporin-9 had no effect in the pineal body. Like in Fig. 4b and f, in Fig. 5 cells were immunoreactive weakly to laminin, or to the dystrophin-dystroglycan components (see Fig. 5b,g, respectively). Other photomicrographs demonstrated basal lamina-components around them, mainly perlecan (Fig. 5h,i). Utrophin (Fig. 5g) and dystrophin were also found in cells.

Discussion

Differences between immunolabelling of pineal and cerebral vessels

The distribution of the components of basal lamina and dystrophin-dystroglycan complex have been investigated extensively in the brain, and our former observations (Bagyura et al., 2007) are in accordance with these data. Therefore, they are cited now from the literature, and have not been displayed in figures repeatedly here.

In the brain, laminin is detectable in the meningeal

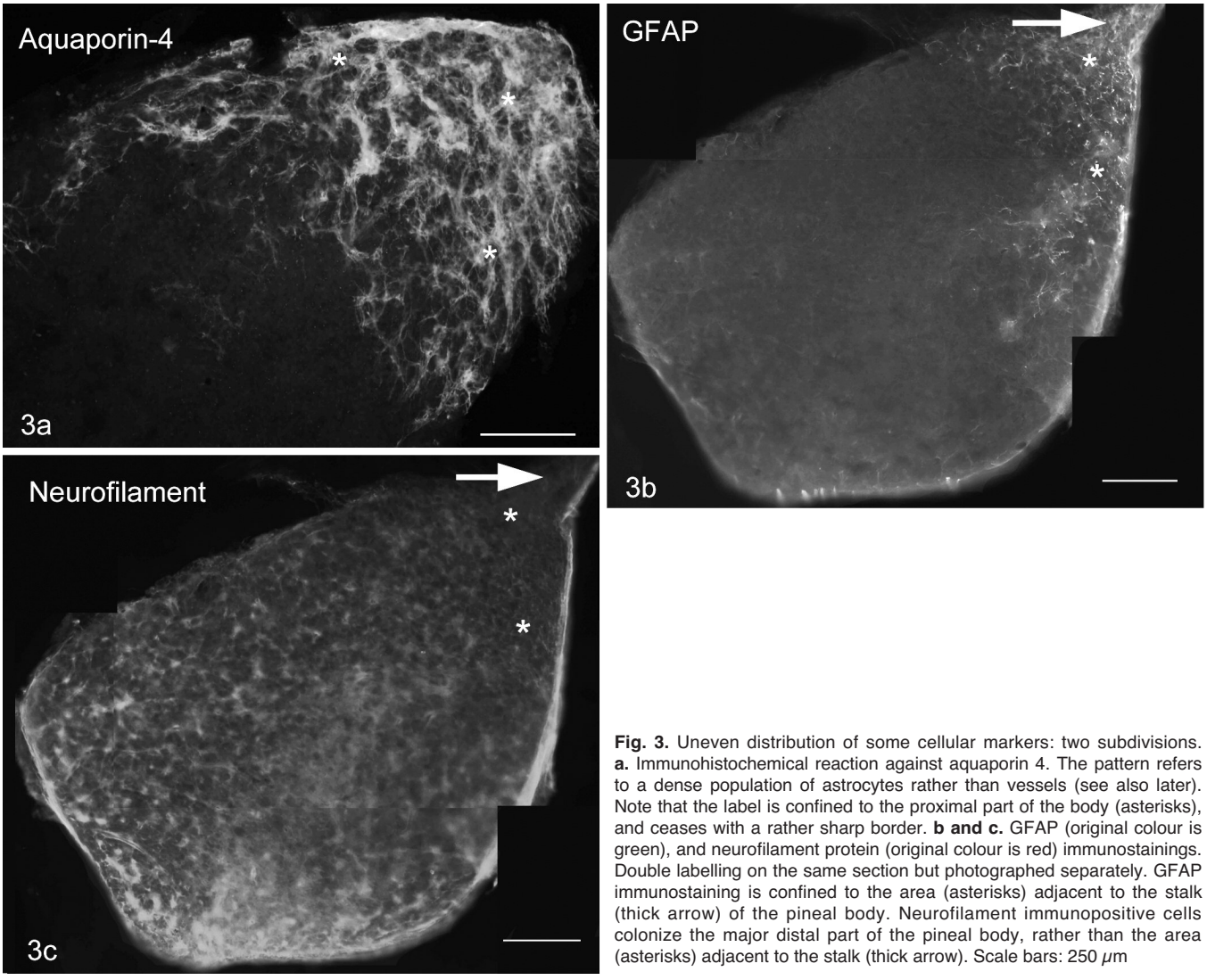

Fig. 3. Uneven distribution of some cellular markers: two subdivisions. **a.** Immunohistochemical reaction against aquaporin 4. The pattern refers to a dense population of astrocytes rather than vessels (see also later). Note that the label is confined to the proximal part of the body (asterisks), and ceases with a rather sharp border. **b and c.** GFAP (original colour is green), and neurofilament protein (original colour is red) immunostainings. Double labelling on the same section but photographed separately. GFAP immunostaining is confined to the area (asterisks) adjacent to the stalk (thick arrow) of the pineal body. Neurofilament immunopositive cells colonize the major distal part of the pineal body, rather than the area (asterisks) adjacent to the stalk (thick arrow). Scale bars: 250 μm

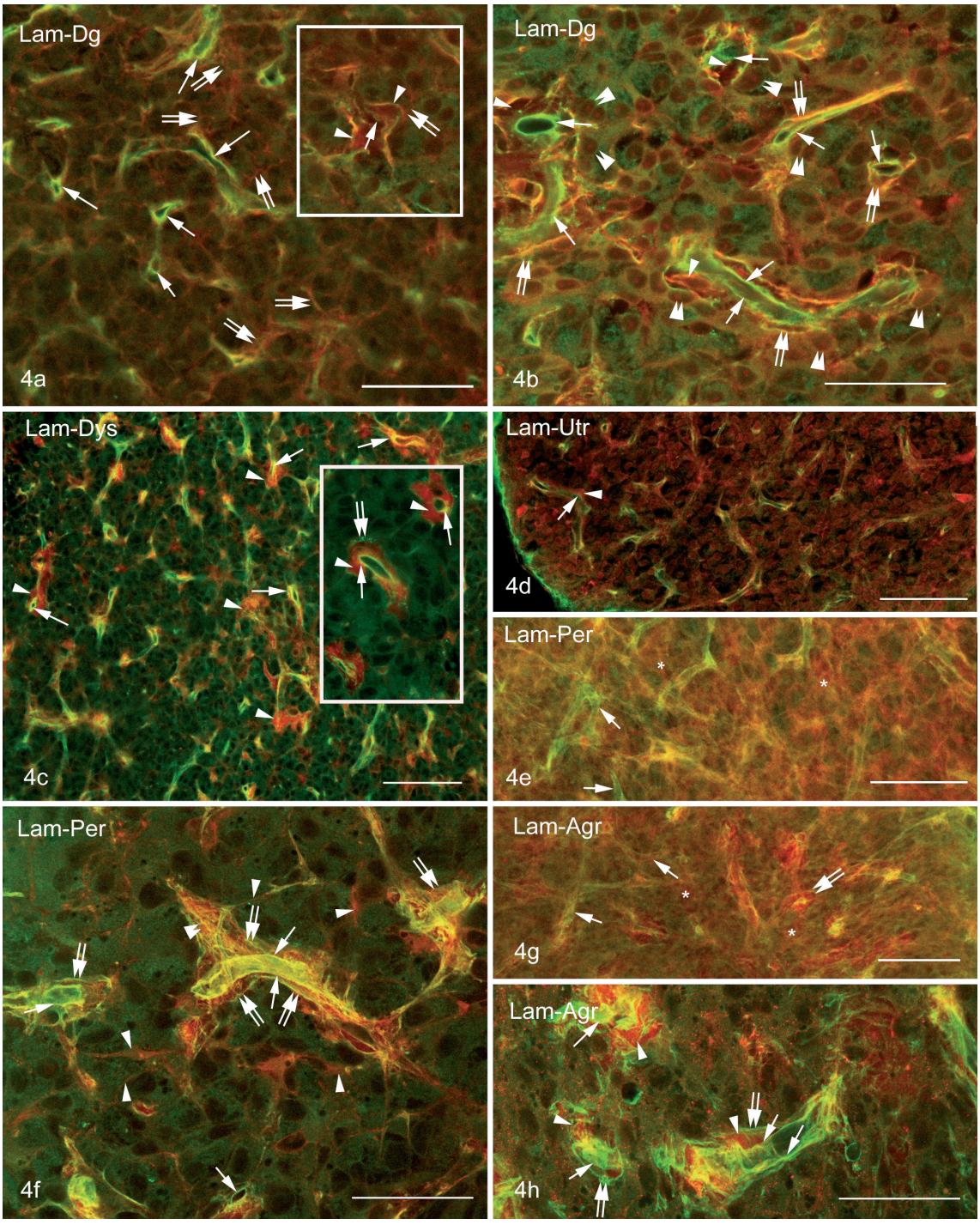

Fig. 4. Connection of vessels and the embedding network. **a.** Double labelling of laminin (green) and dystroglycan (red). In the vessel walls (arrows) laminin predominates, whereas the interconnecting network (double arrows) is visualized mainly by the immunohistochemical reaction against dystroglycan. Yellow colour refers to co-localization. Inset: higher magnification, arrowhead points to an outer, basal lamina-like structure. **b.** Similar labelling as before, a little higher magnification reveals a more complex arrangement. Vessels have a laminin positive inner (arrows), and a yellow, double stained (double arrows) basal lamina. Arrowheads point to a dystroglycan-like, red substance between them. In the background, not only a network, but also cell contours are visible in faint green or red. Some of the latter ones (double arrowheads) are in contact with the outer basal lamina. **c.** Dys2 antibody (red) results in a patchy labelling (arrowheads), which seems to be co-localized with the laminin immunostaining (green) of the vessels only at some points (arrows, yellow). Instead, it is situated on the contraluminar side of the laminin positive layer. Inset: higher magnification, double arrowhead marks a weak outer laminin-positive lamina. **d.** Laminin (green) and utrophin (red) immunostainings. Basal lamina (arrow), with utrophin attached (arrowhead). **e.** Laminin (green) and perlecan (red) immunostainings. Laminin predominates in the vessels (arrows), whereas perlecan immunostaining is more intense in the background (asterisks). **f.** Higher magnification reveals a more complex arrangement. Vessels (arrows) have a yellowish green colour due to the presence of perlecan in addition to the laminin. Double arrows point to an outer basal lamina, arrowheads mark branches of the background network, in which perlecan predominates. Double arrow marks the loose structure of outer lamina, probably around a tangentially sectioned vessel, where no lumina, only the perlecan layer between the inner and outer laminae was in the section plane. **g and h.** Laminin (green) and agrin (red) combination results in similar pictures like the laminin *plus* perlecan does. Arrows point to vessels, double arrows an outer basal lamina around, whereas arrowheads point to the agrin between them. The asterisks mark the background in which agrin predominates to laminin. Agr: agrin; Aq4: aquaporin-4; Dg: dystroglycan; Dy: dystrophin; Gs: glutamine synthetase; Lam: laminin; Nf: neurofilament protein; Per: perlecan; Utr: utrophin. Scale bars: a, 80 μm; b, f, g, 50 μm; c, d, e, h, 100 μm; inset in a, 40 μm; inset in c, 30 μm.

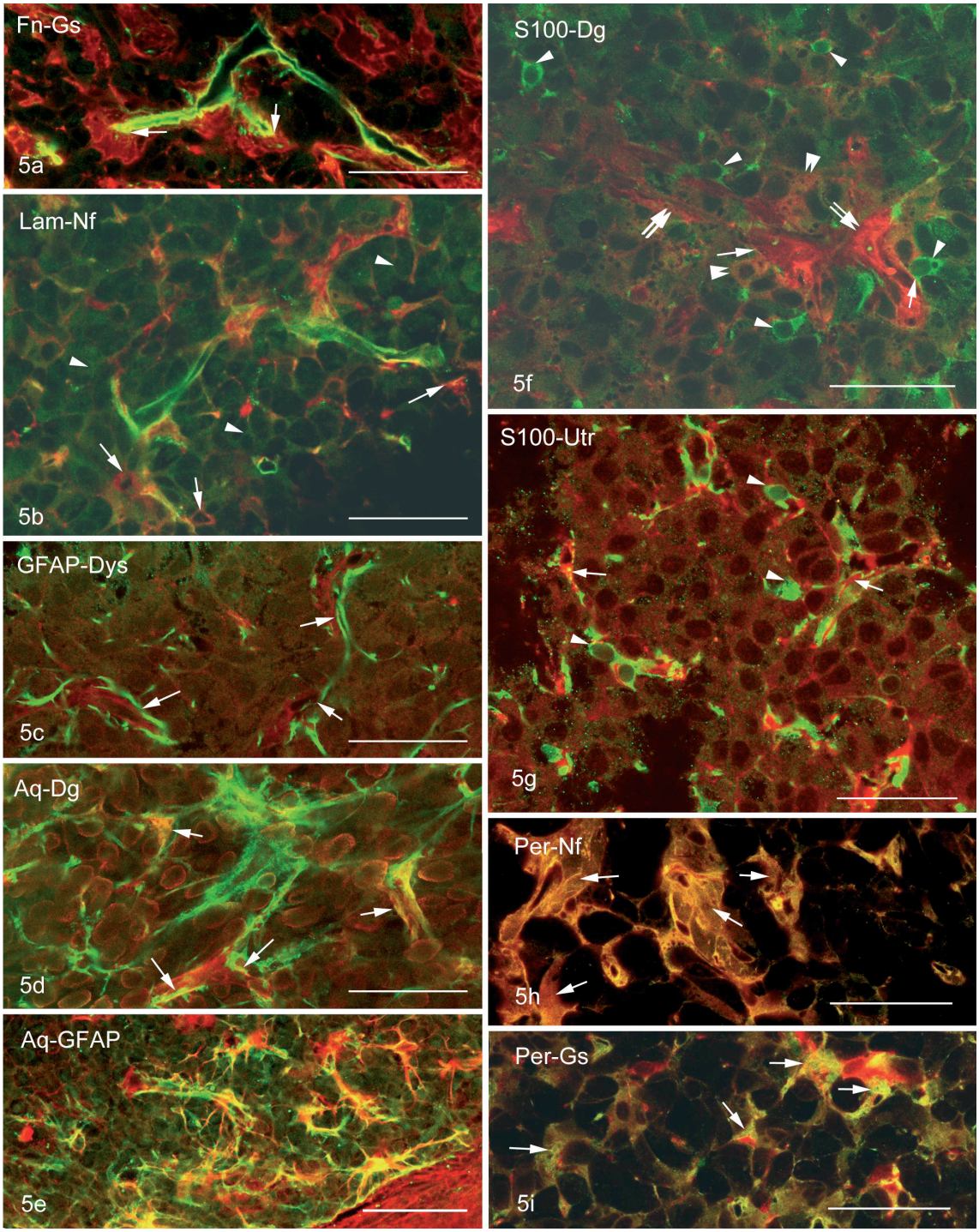

Fig. 5. Cellular elements. **a.** Vascular contact (arrows) of glutamine synthetase immunoreactive cells (red). Vessels were visualized by immunostaining of fibronectin (green). **b.** Vascular contacts of neurofilament immunopositive cells (red, arrows). Vessels were visualized by immunostaining of laminin (green). The background network of laminin and cells is also visible (arrowheads). **c and d.** Astrocytes immunostained against GFAP or aquaporin-4, respectively (green), form contacts (arrows) with vessels immunostained against dystroglycan (red). (Here rabbit anti-GFAP, and FITC-conjugated anti-rabbit immunoglobulin were used). Note the stellate shape of the aquaporin-immunopositive elements. **e.** GFAP immunopositivity (red) at least in part co-localizes (yellow) with aquaporin-4 (green) immunopositivity in astrocytes. Both immunostainings are confined to the area adjacent to the stalk of the pineal body. (Here mouse anti-GFAP, and Cy^3-conjugated anti-mouse immunoglobulin were used). **f.** Double labelling of S100 (cells, arrowheads, green) and dystroglycan (vessels, double arrow, red). Note the co-localization of dystroglycan and S100-protein in some cells (double arrowheads), and the vascular cell contacts (arrows). **g.** S100 positive cells (green, arrowheads) are surrounded by utrophin positive network (red, arrows point to vessel-like structures), in which cells are recognizable. **h.** Perlecan network on neurofilament immunopositive cells (arrows, individual colour is red). Here and in the next case the immunoreaction product of perlecan is green, since it was visualized with FITC-conjugated anti-rat immunoglobulin. Yellow colour refers to co-localization. **i.** Perlecan network (yellowish green) on glutamine synthetase immunopositive cells (arrows, individual colour is red), which form a network (arrows). Agr: agrin; Aq4: aquaporin-4; Dg: dystroglycan; Dy: dystrophin; Gs: glutamine synthetase; Lam: laminin; Nf: neurofilament protein; Per: perlecan; Utr: utrophin. Scale bars: a-d, f-i, 50 μm; e, 100 μm.

vessels, and in the segments of the vessels where they intrude into the brain substance (Virchow-Robin spaces), but not throughout the brain. In brief, the basal lamina between the brain vessels and the perivascular glia is in fact formed by the fusion of two basal laminae: a glial (parenchymal) one, and a vascular one (Bär and Wolff, 1972; Marin-Padilla, 1985; del Zoppo and Hallenbeck, 2000; Sixt et al., 2001; Hallmann et al., 2005). According to several observations, however, laminin immunopositivity can be detected only when the two laminae did not fuse together completely: in the immature vessels, in the entering segments of vessels at the brain surface (Virchow-Robin spaces), and in the circumventricular organs (Shigematsu et al., 1989; Zhou, 1990; Krum et al., 1991; Kálmán et al., 2000; Szabó and Kálmán, 2004, 2008). Otherwise, cerebrovascular laminin immunopositivity is only detectable in frozen sections (Eriksdotter-Nilsson et al., 1986), or following enzyme treatment (Mauro et al, 1984**;** Franciosi et al., 2007). In the pineal gland there is a perivascular space around vessels, with separate continuous vascular basal lamina and a parenchymal basal lamina, which seems to be weaker and somewhat discontinuous. It is in accordance with the electron microscopic data (Vollrath, 1981), and with the opinion that the pineal body is a circumventricular organ, too (Palkovits, 1986; Vígh et al., 2004). Another point of view is that pineal vessels do not originate from cerebral vessels, but directly from meningeal ones (Vollrath, 1981). Note that pineal vessels are less brilliant following laminin immunostaining than the meningeal vessels around the gland.

Cerebral vessels and meningeal glia limitans are immunopositive to ß-dystroglycan according to the findings of Uchino et al. (1996), Zaccaria et al. (2001), Moore et al. (2002), and more recently by Ambrosini et al. (2008) and Szabó and Kálmán (2008), whereas meningeal vessels remain immunonegative. Similar features were found in the pineal gland, but delineation of vessels was less complete than by the immunostaining to laminin, mainly in the midpart of the gland. A meaningful difference was, however, the complete absence of α1-dystrobrevin immunoreactivity from the pineal vessels. Brain vessels can be visualized completely by immunohistochemical reaction to α1-dystrobrevin, whereas ß-dystrobrevin was found in neurons (Blake et al., 1998, 1999; Ueda et al., 2000). Our observations correspond with these data (Bagyura et al., 2007). It is to be noted that dystrobrevins are components of the dystrophin-dystroglycan complex (for references see Introduction), as well as α1-syntrophin, which was also missing from the pineal vessels, although its presence in cerebral vessels has been reported (Haenggi et al., 2004; Bragg et al., 2006; Ambrosini et al., 2008). Neither dystrobrevin nor syntrophin was found in the meningeal vessels. The absence of syntrophin and dystrobrevin cannot be attributed to the circumventricular organ-features of the pineal gland, since other circumventricular organs - e.g. subfornical organ, area postrema - display vascular immunoreactivity to these substances (Bagyura et al., 2007).

Aquaporin 4 - its occurrence is confined, intracellular distribution is different from the cerebral one

In the brain, aquaporin-4 is the predominant aquaporin (Hasegawa et al., 1994; Jung et al., 1994; Frigeri et al., 1995), which occurs mainly in the perivascular glial endfeet, whereas aquaporin-9 was found in the cell bodies and processes (Badaut and Regli, 2004). Aquaporin-4 therefore delineates the walls of cerebral vessels (Nielsen et al., 1997; Goren et al., 2006). In the pineal gland aquaporin-9 was not found at all, but aquaporin-4 decorated both the cell bodies and processes and the endfeet, not densely enough, however, to delineate the courses of the vessels. Aquaporin-4 occurred in a similar area to GFAP, in the proximal part of the pineal gland around the stalk (see also Goren et al., 2006). Syntrophin has been found to be responsible for the concentration of aquaporin-4 to the perivascular glial end-feet (Neely et al., 2001; Amiry-Moghaddam et al., 2003a,b, 2004; Nico et al., 2003, 2004; Warth et al., 2004, 2005), therefore the absence of α1-syntrophin may underlie the even distribution of aquaporin in the astrocytes instead of a perivascular concentration.

Uneven distribution of immunolabelled vessels

Data have been published on the cerebrovascular occurrences of utrophin (Knuesel et al., 2000; Haenggi et al., 2004), agrin (Barber and Lieth, 1997), and also dystrophin in the perivascular glial endfeet (Jancsik and Hajós, 1999; Moukhles and Carbonetto, 2001). In the pineal gland vessels' immunoreactivity to these substances proved to be confined to the proximal end of the body (near the stalk: utrophin, agrin), or to the opposite part (dystrophin). In other areas of the pineal gland they occurred among the parenchymal cells, and formed even 'patchy' deposits on the vessels but did not delineate long vascular segments. It is worth noting that in the brain different amino-terminally truncated dystrophin isoforms were found in addition to the full-length Dp427: Dp140, and Dp71, numbered according to their molecular weight (Lidov, 1996). The anti-dystrophin antibody (Dys2, Novocastra) applied by us, however, recognizes the C-terminals, which is uniform in these isoforms (Jancsik and Hajós, 1999). The different occurrence of utrophin and dystrophin is not surprising since they are autosomal homologues, and have the same task in the dystrophin-dystroglycan complex; therefore they usually substitute each other (Knuesel et al., 2000). It is to be noted that in other circumventricular organs - e.g. subfornical organ, area postrema - vessels proved to be immunopositive to agrin and utrophin (Bagyura et al., 2007).

Type-I collagen and fibronectin were also found in

the distal end of the body, where vessels enter from the meninx, but only near the surface, since they represent perivascular connective tissue rather than basal lamina. Although pineal vessels are usually described to enter on the distal end of the gland (Quay, 1973; Vollrath, 1981) demonstrated a link to the choroid plexus at the proximal end. The agrin and utrophin immunopositivity may be related to the vessels connected to this system.

Network and cells

Another difference between the pineal and cerebral tissues is that in the brain there is no background 'network' from basal lamina components around and between the vessels. No "wing-like" protrusions interconnecting cerebral vessels have been described, except for one similar system: Mercier et al. (2002, 2003) found a delicate network formed by laminin, which originates from the basal lamina of capillaries near the ventricular surface. It spans the subependymal layer and sends off branches to the ependyma in a fashion quite similar to the fractal system. For this reason it was termed 'fracton'.

The photomicrographs give the impression that in the pineal gland the basal lamina components, as well as dystroglycan, dystrophin, and utrophin form a network independent from cells. Since cell bodies are labelled poorly, the cellular origin of these components remains obscure. In some pictures, however, faint cell contours are visible. The combination of these labellings with cell markers can reveal a connection between the basal lamina components and the cells.

Surprising observations were the 'patchy' deposition of agrin, perlecan, dystrophin, and utrophin (Figure 4c-h), and their position between the two basal laminae (the parenchymal and the vascular ones). Especially, the intracellular dystrophin and utrophin were not expected in this position. Pineal cells immunostained with glutamine synthetase, S100-protein or neurofilament protein formed contacts on the vessels.

Cell types and subdivisions in the gland

Previous investigations detected glial markers in the so-called interstitial cells: S100 protein (Møller et al., 1978b; Calvo et al. 1988; López-Muñoz et al., 1992a,b), glutamine synthetase (Krstic' and Nicolas, 1992), vimentin (López-Muñoz et al., 1992a; Sakai et al., 1996). The latter authors consider the interstitial cells to be immature astrocytes. GFAP- immunopositive cells were only found in the proximal part of the body (López-Muñoz et al., 1992a,b). Min et al. (1987) detected neuron-specific enolase in some cells. Our findings are in accordance with these results, but contribute the fact that the neurofilament protein immunopositive cells occur mainly in the distal two-third of the gland, i.e. which is free or almost free of GFAP-immunopositive cells, although the border is not clear, since there is a mixed population in-between. GFAP- and aquaporin 4 immunopositive cells occurred in similar areas, and at least in part of them the immunostainings were co-localized. Including the uneven distribution of vessels visualized by immunohistochemical reaction to agrin and utrophin on one hand, and to dystrophin on the other hand, these differences suggest a tendency of separation of two subdivisions, a proximal third and a distal two-third. S100 and glutamine synthetase immunopositive cells were evenly distributed. Representatives of either cell type were found in vascular contacts.

Conclusions

In conclusion, the investigated substances display different immunohistochemical patterns in the pineal and in the cerebral vessels. The main differences are that the pineal vessels are immunoreactive to laminin, but immunonegative to α1-dystrobrevin, in contrast to the cerbral ones. The laminin immunopositivity, as well as the double basal lamina around the pineal vessels may be attributed to the fact that the pineal gland is a circumventricular organ, without blood-brain barrier. In contrast to the brain tissue, the pineal gland is enmeshed by a network of basal lamina components. There are differences in the vascular immunohistochemical patterns observed in the proximal and distal parts of the gland. Aquaporin-4 was confined to the proximal part, and its immunoreactivity seemed to delineate astrocytes rather than vessels, in contrast to brain tissue. The functional or other reasons of these latter observations remained to be explained.

Acknowledgements. The study was supported by the fund OTKA 60930/2006, holder M. Kálmán.

References

Agre P. and Kozono D. (2003). Aquaporin water channels: molecular mechanisms for human diseases. FEBS Lett. 555, 72-78.

Agre P., King L.S., Yasui M., Guggino W.B., Ottersen O.P., Fujiyoshi Y., Engel A. and Nielsen S. (2002). Aquaporin water channels from atomic structure to clinical medicine. J. Physiol. 542, 3-16.

Ambrosini E., Serafini B., Lanciotti A., Tosini F., Scialpi F., Psaila R., Raggi C., Di Girolamo F., Petrucci T.C. and Aloisi F. (2008). Biochemical characterization of MLC1 protein in astrocytes and its association with the dystrophin-glycoprotein complex. Mol. Cell. Neurosci. 37, 480-493.

Amiry-Moghaddam M., Otsuka T., Hurn P.D., Traystman R.J., Haug F-M., Froehner S.C., Adams M.E., Neely J.D., Agre P., Ottersen O.P. and Bhardwaj A. (2003a). An α-syntrophin-dependent pool of AQP4 in astroglial end-feet confers bidirectional water flow between blood and brain. Proc. Natl. Acad. Sci. USA 100, 2106-2111.

Amiry-Moghaddam M., Williamson A., Palomba M., Eid T., de Lanerolle N.C., Nagelhus E.A., Adams M.E., Froehner SC., Agre P. and Ottersen O.P. (2003b). Delayed K^+ clearance associated with aquaporin-4 mislocalization: phenotypic defects in brains of alpha-synrophin-null mice. Proc. Natl. Acad. Sci. USA. 100, 13615-13620

Amiry-Moghaddam M., Frydenlund D.S. and Ottersen O.P. (2004). Anchoring of aquaporin-4 in brain: molecular mechanisms and implications for the physiology and pathophysiology of water transport. Neuroscience 129, 999-1010.

Badaut J. and Regli L. (2004). Distribution and possible roles of aquaporin 9 in the brain. Neuroscience 129, 971-981.

Bagyura Z., Adorján I., Pócsai K. and Kálmán M. (2007). Functional relevance of the immunoreactivity of basal lamina components and laminin receptors - a study in rat brain. I. Vessels and meninges of intact adult brain. Clin. Neurosci. 60, Suppl 1, 7.

Barber A.J. and Lieth E. (1997). Agrin accumulates in the brain microvascular basal lamina during development of the blood-brain barrier. Dev. Dyn. 208, 62-74.

Bär T.H. and Wolff J.R. (1972). The formation of capillary basement membranesduringinternal vascularization of the rat's cerebral cortex. Z. Zellforsch. 133, 231-248.

Blake D.J., Nawrotzki R., Loh N.Y., Gorecki D.C. and Davies K.E. (1998). ß-dystrobrevin, a member of the dystrophin-related protein family. Proc. Natl. Acad. Sci. USA 95, 241-246.

Blake D.J., Hawkes R., Benson M.A. and Beesley P.W. (1999). Different dystrophin-like complexes are expressed in neurons and glia. J. Cell Biol. 147, 645-658.

Bragg A.D., Amiry-Moghaddam M., Ottersen O.P., Adams M.E. and Froehner S.C. (2006). Assembly of a perivascular astrocyte protein scaffold at the mammalian blood-brain barrier is dependent on alpha-syntrophin. Glia. 53, 879-890.

Calvo J., Boya J., Borregon A. and Garcia-Mauriño J.E. (1988). Presence of glial cells in the rat pineal gland: a light and electron microscopic immunohistochemical study. Anat. Rec. 220, 424-428.

Chamberlain J. (1999). The dynamics of dystroglycan. Nat. Genet. 23, 256-8.

Colognato H. and Yurchenko P.D. (2000). Form and function: The laminin family of heterotrimers. Dev. Dyn. 218, 213-231.

Culligan K. and Ohlendieck K. (2002). Diversity of the Brain Dystrophin-Glycoprotein Complex. J. Biomed. Biotechnol. 2, 31-36.

del Zoppo G.J. and Hallenbeck J.M. (2000). Advances in the vascular pathophysiology of ischemic stroke. Thromb. Res. 98, 73-81.

Durbeej M., Henry M.D. and Campbell K.P. (1998a). Dystroglycan in development and disease. Curr. Opin. Cell Biol. 10, 594-601.

Durbeej M., Henry M.D., Ferletta M., Campbell K.P. and Ekblom P. (1998b). Distribution of dystroglycan in normal adult mouse tissues. J. Histochem. Cytochem. 46, 449-457.

Ehmsen J., Poon E. and Davies K. (2002). The dystrophin-associated protein complex. J. Cell. Sci. 115, 2801-3.

Eriksdotter-Nilsson M., Björklund H. and Olson L. (1986). Laminin immunohistochemistry is a simple method to visualize and quantitate vascular structures in the mammalian brain. J. Neurosci. Meth. 17, 275-286.

Franciosi S., De Gasperi R., Dickstein D.L., English D.F., Rocher A.B., Janssen W.G., Christoffel D., Sosa M.A., Hof P.R., Buxbaum J.D. and Elder G.A. (2007). Pepsin pretreatment allows collagen IV immunostaining of blood vessels in adult mouse brain. J. Neurosci. Methods. 163, 76-82.

Frigeri A., Gropper M.A., Umenishi F., Kawashima M. and Brown D. (1995). Localization of MIWC and GLIP water channel homologs in neuromuscular, epithelial and glandular tissues. J. Cell. Sci. 108, 2993-3002.

Ganguly S., Coon S.L. and Klein D.C. (2002). Regulation of melatonin biosynthesis in the mammalian pineal organ. Cell Tissue Res. 309, 139-150.

Goren O., Adorján I. and Kálmán M. (2006). Heterogeneous occurrence of aquaporin-4 in the ependyma and in the circumventricular organs in rat and chicken. Anat. Embryol. 211, 155-72.

Haenggi T., Soontornmalai A., Schaub M.C. and Fritsch J-M. (2004). The role of utrophin and Dp71 for assemgly of different dystrophin-associated protein complexes (DPCs) in the choroid plexus and microvasculature of the brain. Neuroscience 129, 403-413.

Hallmann R., Horn N., Selg M., Wendler O., Pausch F. and Sorokin L.M. (2005). Expression and function of laminins in the embryonic and mature vasculature. Physiol. Rev. 85, 979-1000.

Hasegawa H., Ma T., Skach W., Matthay M.A. and Verkman A.S. (1994). Molecular cloning of a mercurial- insensitive water channel expressed in selected water-transporting tissues. J. Biol. Chem. 269, 5497-5500.

Heidbüchel U. and Vollrath L. (1983). Pineal complex of rats: Effects of superficial pinealectomy on the deep pineal. Acta Anat. 117, 165-169.

Henry M.D. and Campbell K.P. (1996). Dystroglycan: an extracellular matrix receptor linked cytoskeleton. Curr. Opin. Cell Biol. 8, 625-631.

Ibraghimov-Beskrovnaya O., Ervasti J.M., Leveille C.J., Slaughter C.A., Sernett S.W. and Campbell K.P. (1992). Primary structure of dystrophin-associated glycoproteins linking dystrophin to the extracellular matrix. Nature 355, 696-702.

Jancsik V. and Hajós F. (1999). The demonstration of immunoreactive dystrophin and its developmental expression in perivascular astrocytes. Brain Res. 831, 200-205.

Jung J.S., Bhat R.V., Predston G.M., Guggino W.B., Baraban J.M. and Agre P. (1994). Molecular characterization of an aquaporin cDNA from brain: candidate osmoreceptor and regulator of water balance. Proc. Natl. Acad. Sci. USA 91, 13052-13056.

Kálmán M., Kiss B. and Szabó A. (2000). Investigation of brain vascularisation by immunohistochemical staining against laminin. Neurobiology 8, 342-343.

Knuesel I., Bornhauser B.C., Zuellig R.A., Heller F., Schaub M.C. and Fritschy J.M. (2000). Differential expression of utrophin and dystrophin in CNS neurons: an in situ hybridization and immunohistochemical study. J. Comp. Neurol. 422, 594-611.

Krstiç R. and Nicolas D. (1992). Light and electron microscopic immunocytochemical localization of glutamine synthetase in the superficial pineal gland of the rat. Acta Histochem. 93, 382-387.

Krum J.M., More N.S. and Rosenstein J.M. (1991). Brain angiogenesis: variations in vascular basement membrane glycoprotein immunoreactivity. Exp. Neurol. 111, 151-165.

Lerner A.B., Case J.D. and Heinzelman R.V. (1959). Structure of melatonin. Chem. Soc. 81, 6084-6085.

Libby R.T., Champliaud M.F., Claudepierre T., Xu Y., Gibbons P.E., Koch M., Burgeson R.E., Hunter D.D. and Brunken W.J. (2000). Laminin expression in adult and developing retinae: Evidence of two novel laminins. J. Neurosci. 20, 6517-6528.

Lidov H.G.W. (1996). Dystrophin in the nervous system. Brain Pathol. 6, 63-77.

López-Muñoz F., Boya J., Calvo J.L. and Marín F. (1992a). Coexpression of vimentin and glial fibrillary acidic protein in glial cells of the adult rat pineal gland. J. Pineal Res. 12, 145-148.

López-Muñoz F., Boya J., Calvo J.L. and Marín F. (1992b). Immunohistochemical localization of glial fibrillary acidic protein (GFAP) in rat pineal stalk astrocytes. Histol. Histopathol. 7, 643-6.

Marin-Padilla M. (1985). Early vascularization of the embryonic cerebral

cortex: Golgi and electron microscopic studies. J. Comp. Neurol. 241, 237-249.

Mauro A., Bertolotto A., Germano I., Giaccone G., Giordana M.T., Migheli A. and Schiffer D. (1984). Collagenase in the immunohistochemical demonstration of laminin, fibronectin and factor VIII/Rag. Histochemistry. 80, 157-163.

Mercier F., Kitasako J.T. and Hatton G.I. (2002). Anatomy of the brain neurogenic zones revisited: fractones and the fibroblast/macrophage network. J. Comp. Neurol. 451, 170-88.

Mercier F., Kitasako J.T. and Hatton G.I. (2003). Fractones and other basal laminae in the hypothalamus. J. Comp. Neurol. 455, 324-340.

Min K.W., Seo I.S. and Song J. (1987). Postnatal evolution of the human pineal gland. An immunohistochemical study. Lab. Invest. 57, 724-8.

Moore S.A., Salto F., Chen N., Michele D.E., Henry M.D., Messing A., Cohn R.D., Ross-Barta S.E., Westra S., Williamson R.A., Hoshi T. and Campbell K.P. (2002). Deletion of brain dystroglycan recapitulates aspects of congenital muscular dystrophy. Nature 418, 422-425.

Moukhles H. and Carbonetto S. (2001). Dystroglycan contributes to the formation of multiple dystrophin-like complexes in brain. J. Neurochem. 78, 824-834.

Møller M. and Baeres F.M. (2002). The anatomy and innervation of the mammalian pineal gland. Cell Tissue Res. 309, 139-150.

Møller M. and Veen T. van (1981). Vascular permeability in the pineal gland of the Mongolian gerbil and the Djungarian hamster. In: Human reproduction. Semm K. and Mettler L. (eds). Intern Congr. Series 551. Elsevier/North-Holland. Amsterdam. pp 539-543.

Møller M., Deurs B. van and Westergård E. (1978a). Vascular permeability to proteins and peptides in the mouse pineal gland. Cell Tissue Res. 195, 1-15.

Møller M., Ingild A. and Bock E. (1978b). Immunohistochemical demonstration of S100 protein and GFA protein in interstitial cells of rat pineal gland. Brain. Res. 140, 1-13.

Neely J.D., Amiry-Moghaddam M., Ottersen O.P., Froehner S.C., Agre P. and Adams M.E. (2001). Syntrophin-dependent expression and localization of aquaporin-4 water-channel protein. Proc. Natl. Acad. Sci. USA 98, 14108-14113.

Nico B., Frigeri A., Nicchia G.P., Quondamatteo F., Herken R., Errede M., Ribatti D., Svelto M. and Roncali L. (2001). Role of aquaporin-4 water channel in the development and integrity of the blood-brain barrier. J. Cell Sci. 114, 1297-1307.

Nico B., Frigeri A., Nicchia G.P., Corsi P., Ribatti D., Quondamatteo F., Herken R., Girolamo F., Marzullo A., Svelto M. and Roncali L. (2003). Severe alterations of endothelial and glial cells in the blood-brain barrier of dystrophic mdx mice. Glia 42, 235-251.

Nico B., Nicchia G.P., Frigeri A., Corsi P., Mangieri D., Ribatti D., Svelto M. and Roncali L. (2004). Altered blood-brain barrier development in dystrophic MDX mice. Neuroscience 125, 921-935.

Nielsen S., Nagelhus E.A., Amiry-Moghaddam M., Bourque C., Agre P. and Ottersen O.P. (1997). Specialized membrane domains for water transport in glial cells: high-resolution immunogold cytochemistry of aquaporin-4 in rat brain. J. Neurosci. 17, 171-80.

Palkovits M. (1986). Summary of structural and functional aspects of the circumventricular organs. In: Circumventricular organs and body fluids. Vol. II. Gross P.M. (ed). CRC Press Inc. Boca Raton, Florida. pp 209-218.

Quay W.B. (1973). Retrograde perfusion of the pineal region and the question of pineal vascular routes to brain and choroid plexuses. Am. J. Anat. 137, 387-402.

Sakai Y., Hira Y. and Matsushima S. (1996). Regional differences in the pineal gland of the cotton rat, *Sigmodon hispidus*: light microscopic, electron microscopic, and immunohistochemical observations. J. Pineal Res. 20, 125-127.

Shigematsu K., Kamo H., Akiguchi J., Kameyama M. and Kimura H. (1989). Neovascularization of transplanted central nervous tissue suspensions: an immunohistochemical study with laminin. Neurosci. Lett. 99, 18-23.

Sixt M., Engelhardt B., Pausch F., Hallman R., Wendler O. and Sorokin L.M. (2001). Endothelial cell laminin isoforms, laminin 8 and 10, play decisive roles in T cell recruiment across the blood-brain barrier in experimental autoimmun encephalomyelitis. J. Cell Biol. 153, 933-945.

Smalheiser N.R. and Kim E. (1995). Purification of cranin, a laminin binding membrane protein. Identity with dystroglycan and reassessment of its carbohydrate moieties. J. Biol. Chem. 270, 15425-33.

Suzuki T. and Kachi T. (1995). Immunohistochemical studies on supporting cells in the adrenal medulla and pineal gland of adult rat, especially on S-100 protein, glial fibrillary acidic protein and vimentin. Kaibogaku Zasshi. 70, 130-9.

Szabó A. and Kálmán M. (2004). Disappearance of the post-lesional laminin immunopositivity of brain vessels is parallel with the formation of gliovascular junctions and common basal lamina. A double-labeling immunohistochemical study. Neuropathol. Appl. Neurobiol 30, 169-170.

Szabó A. and Kálmán M. (2008). Post traumatic lesion absence of beta-dystroglycan-immunopositivity in brain vessels coincides with the glial reaction and the immunoreactivity of vascular laminin. Curr. Neurovasc. Res. 5, 206-13.

Tian M., Jacobson C., Gee S.H., Campbell K.P., Carbonetto S. and Jucker M. (1996). Dystroglycan in the cerebellum is a laminin α2-chain binding protein at the glial-vascular interface and is expressed in Purkinje cells. Eur. J. Neurosci. 8, 2739-2747.

Uchino M., Hara A., Mizuno Y., Fujiki M., Nakamura T., Tokunaga M., Hirano T., Yamashita T., Uyama E., Ando Y., Mita S. and Ando M. (1996). Distribution of dystrophin and dystrophin-associated protein 43DAG (beta-dystroglycan) in the central nervous system of normal controls and patients with Duchenne muscular dystrophy. Intern. Med. 35, 189-94.

Ueda H., Baba T., Terada N., Kato Y., Fujii Y., Takayama I., Mei X. and Ohno S. (2000). Immunolocalization of dystrobrevin int he astrocytic endfeet and endothelial cells in the rat cerebellum. Neurosci. Lett. 283, 121-124.

Vajda Z., Pedersen M., Füchtbauer E-M., Wertz K., Stødkilde-Jørgensen H., Sulyok E., Dóczi T., Neely J.D., Agre P., Frøkiaer J. and Nielsen S. (2002). Delayed onset of brain edema and mislocalization of aquaporin-4 in dystrophin-null transgenic mice. Proc. Natl. Acad. Sci. USA 99, 13131-13136.

Venero J.L., Vizuete M.L., Machado A. and Cano J. (2001). Aquaporins in the central nervous system. Prog. Neurobiol. 63, 321-336.

Vígh B., Manzano e Silva M.J., Frank C.L., David C., Czirok S.J., Vincze C., Rácz G., Lukáts A. and Szél Á. (2004). The circumventricular organs of the brain: Do they represent a cerebrospinal fluid-dependent regulatory system? Med. Hypotheses Res. 1, 77-100.

Vollrath L. (1981). The pineal organ. In: Handbuch der mikroskopischen Anatomie des Menschen. Vol VI/7. Oksche A. and Vollrath L. (eds). Springer. Berlin, Heidelberg, New York. pp 1-665.

Warth A., Mittelbronn M. and Wolburg H. (2004). Redistribution of aquaporin-4 in human glioblastoma correlates with loss of agrin immunoreactivity from brain capillary basal laminae. Acta Neuropathol. 107, 311-318.

Warth A., Mittelbronn M. and Wolburg H. (2005). Redistribution of the water channel protein aquaporin-4 and the K^+ channel protein Kir4.1 differs in low- and high-grade human brain tumors. Acta Neuropathol. 109, 418-26.

Welsh M.G. and Beitz A.J. (1981) Modes of protein and peptide uptake in the pineal gland of the Mongolian gerbil: an ultrastructural study. Am. J. Anat. 162, 343-355.

Zaccaria M.L., Di Tommaso F., Brancaccio A., Paggi P. and Petrucci T.C. (2001). Dystroglycan distribution in adult mouse brain: a light and electron microscopy study. Neuroscience 104, 311-24.

Zhou F.C. (1990). Four patterns of laminin-immunoreactive structure in developing rat brain. Dev. Brain Res. 55, 191-201.

Accepted July 6, 2009